



Published in final edited form as:

*Eur J Med Chem.* 2017 February 15; 127: 87–99. doi:10.1016/j.ejmech.2016.12.027.

## Design and synthesis of formononetin-dithiocarbamate hybrids that inhibit growth and migration of PC-3 cells via MAPK/Wnt signaling pathways

Dong-Jun Fu<sup>a,1</sup>, Li Zhang<sup>a,1</sup>, Jian Song<sup>a,1</sup>, Ruo-Wang Mao<sup>a</sup>, Ruo-Han Zhao<sup>a</sup>, Ying-Chao Liu<sup>a</sup>, Yu-Hui Hou<sup>a</sup>, Jia-Huan Li<sup>a</sup>, Jia-Jia Yang<sup>a</sup>, Cheng-Yun Jin<sup>a</sup>, Ping Li<sup>a</sup>, Xiao-Lin Zi<sup>c</sup>, Hong-Min Liu<sup>a</sup>, Sai-Yang Zhang<sup>b,\*</sup>, and Yan-Bing Zhang<sup>a,\*\*</sup>

<sup>a</sup>School of Pharmaceutical Sciences & Collaborative Innovation Center of New Drug Research and Safety Evaluation, Zhengzhou University, Zhengzhou 450001, China

<sup>b</sup>School of Basic Medical Sciences, Zhengzhou University, Zhengzhou 450001, China

<sup>c</sup>Pathology and Laboratory Medicine, University of California, Irvine, Orange, CA 92868, USA

### Abstract

A series of novel formononetin-dithiocarbamate derivatives were designed, synthesized and evaluated for antiproliferative activity against three selected cancer cell line (MGC-803, EC-109, PC-3). The first structure-activity relationship (SAR) for this formononetin-dithiocarbamate scaffold is explored in this report with evaluation of 14 variants of the structural class. Among these analogues, *tert*-butyl 4-(((3-((3-(4-methoxyphenyl)-4-oxo-4*H*-chromen-7-yl)oxy)propyl)thio)carbonothioyl)piperazine-1-carboxylate (**8i**) showed the best inhibitory activity against PC-3 cells (IC<sub>50</sub> = 1.97 μM). Cellular mechanism studies elucidated **8i** arrests cell cycle at G1 phase and regulates the expression of G1 checkpoint-related proteins in concentration-dependent manners. Furthermore, **8i** could inhibit cell growth via MAPK signaling pathway and inhibit migration via Wnt pathway in PC-3 cells.

### Keywords

Formononetin; Dithiocarbamate; Growth; Migration

## 1. Introduction

Natural products have played prominent roles for drug discovery and cancer therapy [1]. Formononetin **1**, a bioactive isoflavone found in red clover plant and widespread in the Leguminosae family, was reported to have many potent pharmacological activities, including antioxidant, antiviral, antitumor, antihypertensive, antibacterial, antiangiogenic effects and so on [2–6]. In recent years, many formononetin analogues were designed as antitumor

\*Corresponding author. celeron16@163.com (S.-Y. Zhang). \*\*Corresponding author. , zhangyb@zzu.edu.cn (Y.-B. Zhang).

<sup>†</sup>These authors contributed equally to this work.

### Appendix A. Supplementary data

Supplementary data related to this article can be found at <http://dx.doi.org/10.1016/j.ejmech.2016.12.027>.

agents and explored their biological mechanism against different human cancer cell lines [7–9]. Its 7-phosphoramidate derivative **2** significantly induced early apoptosis in HepG-2 cells [10]. Formononetin nitrogen mustard derivative **3** could induce cell cycle arrest at G2/M phase and cell apoptosis [11], with an IC<sub>50</sub> value of 3.8 μM against HCT-116 cells (Fig. 1).

Dithiocarbamate, a privileged scaffold in drug discovery with a wide array of biological activities, including antifungal, antibacterial, antitumor, inhibition of carbonic anhydrase activities and so on [12–17]. Besides, the dithiocarbamate has always been used as a linkage to combine different antiproliferative active scaffolds to design new chemical entities. Our group have reported three series of dithiocarbamates derivatives as potential antitumor agents: the butenolide-containing dithiocarbamate **4** displayed an excellent activity against Hela cells with an IC<sub>50</sub> value of 0.77 μM [18]; the novel dithiocarbamate-chalcone analogue **5** could change the expression of apoptosis-related proteins and arrest the cell cycle at G0/G1 phase against SK-N-SH cells [19]; triazole-dithiocarbamate based selective lysine specific demethylase 1 inactivator **6** inhibited gastric cancer cell growth, invasion, and migration (Fig. 2) [20].

Molecular hybridization is a useful strategy of rational design of new ligands based on the recognition of pharmacophoric subunits in the molecular structure of two or more known bioactive derivatives [21]. These above interesting findings and our continuous quest to identify more potent anticancer agents, led to the molecular hybridization of formononetin and dithiocarbamate to integrate them in one molecular platform to generate a new hybrid with an excellent antiproliferative activity (Fig. 3).

As shown in Fig. 3, a molecular hybridization strategy based on the structures of a natural formononetin **1** and a bioactive dithiocarbamate analogue **6** yielded a scaffold which has four parts: (i) a dithiocarbamate group with drug-like properties, (ii) a natural formononetin scaffold as an antitumor pharmacophore fragment (iii) a medium-chain alkoxy group for lipophilicity, and (IV) various aliphatic amine units attached with dithiocarbamate fragment. To the best of our knowledge, there have been no literature reports regarding formononetin-dithiocarbamate hybrids so far. These findings have encouraged us to investigate the potential synergistic effect of dithiocarbamate and formononetin scaffolds.

## 2. Results and discussion

### 2.1. Chemistry

The synthetic route were shown in Scheme 1. Commercially available formononetin **1** was subjected to etherification reaction with 1,2-dibromoethane, 1,3-dibromopropane, 1,4-dibromobutane, or 1,5-dibromopentane to afford **7a–d** in the presence of potassium carbonate. The target analogues were easily obtained in high yields with the mature reaction conditions developed by our group [22].

### 2.2. Antiproliferative activity

In continuation with our efforts toward the identification of novel derivatives with anticancer potential, we evaluated the antiproliferative activity of formononetin analogues **7a–d** and formononetin-dithiocarbamate hybrids **8a–j** against several cancer cell lines (PC-3,

MGC-803 and EC-109) using the MTT assay. Due to potentially similar mode of action between reported dithiocarbamate derivatives and well-known 5-fluorouracil (5-FU), 5-Fu was used as the reference drug in the MTT assay [23]. Besides, formononetin **1** also was a positive control.

The antiproliferative activity results against all three cancer cells for the candidate compounds were shown in Table 1. The replacement of the bromine atom by the dithiocarbamate scaffold resulted in a powerful improvement of activity for formononetin-dithiocarbamate derivatives compared with the corresponding formononetin analogues (**7a–d**). Especially, compound **8i** showed the inhibitory effect against PC-3 cell line with an IC<sub>50</sub> value of 1.97 μM (>30-fold and 15-fold more potent than **7b** and **5-Fu**, respectively). This result suggests that dithiocarbamate moiety may play a synergistic role in determining activity.

In order to complete the SAR study, a series of formononetin-dithiocarbamate hybrids were prepared and evaluated for their antiproliferative activity. With the exception of compounds **8a–j**, all the compounds bearing a dithiocarbamate moiety exhibit antiproliferative activity with IC<sub>50</sub> values ranging from 1.97 to 53.95 μM. To determine whether the amine unites have an effect on the activity, compounds with a piperazine unit (**8a–d**, **8g**), a morpholine unit (**8e**), and a pyrrolidine unit (**8f**) were synthesized. Replacement of the pyrrolidine unit (**8f**) with a morpholine unit (**8e**) led to a decrease of the activity. However, changing the pyrrolidine unit (**8f**) to a 1-methylpiperazine unit (**8d**) led to a significant improvement of the activity against all the tested cell lines. All these results indicated that the piperazine unit may play an important role for their inhibitory activity.

Furthermore, the importance of substituents on the piperazine unit was investigated. Replacing the methyl (**8d**) group by benzyl group (**8a**), ethyl (**8b**), pyridine (**8g**), or acetyl (**8c**) caused a decrease of activity. Removing the *tert*-butyloxycarbonyl group was clearly detrimental for the activity, such as compound **8i** compared to **8d**. The modifications and SAR studies revealed that the *tert*-butyloxycarbonyl group is important for their inhibitory activity.

To investigate whether the length of carbon linker between the formononetin scaffold and the dithiocarbamate scaffold might affect the antiproliferative activity, compounds possessing a *tert*-butyl piperazine-1-carboxylate moiety (**8h–j**) were synthesized. With either extension or reduction of the carbon linker length by one carbon, the antiproliferative activity was decreased (**8i VS. 8h or 8j**). These results suggested that the linker between the formononetin and the dithiocarbamate scaffold plays a significant role in their activities.

Compound **8i** was further examined for possible cytotoxicity against GES-1 (normal human gastric epithelial cell line). We found that compound **8i** exhibited no cytotoxicity against GES-1 (>100 μM). The results indicated that compound **8i** had good selectivity between the selected cancer cell line (MGC-803) and a normal cell line (GES-1). The detailed illustration for SAR of target derivatives was shown in Fig. 4.

### 2.3. Cell viability test and cell growth curve

Based on the screening activity results of all synthetic derivatives, the most potent formononetin-dithiocarbamate hybrid, **8i**, was prioritized to perform further experiment for evaluating its antiproliferative potential in PC-3 cells (Fig. 5). As shown in Fig. 5A, following treatment with **8i**, the viability of the PC-3 cells decreased in a concentration-dependent manner. As shown in cell growth curve (Fig. 5B), the PC-3 cells treated by **8i** began to grow slower than control after 6 h, and the difference of growth speed became significant after 12 h. These results suggested that **8i** could significantly inhibit growth of PC-3 cells.

### 2.4. Clone assays

Based on the most excellent activity against PC-3 cells, compound **8i** was chosen to perform colony formation to investigate whether **8i** could inhibit PC-3 cells proliferation (Fig. 6A and B). The assay measures the ability of PC-3 cells to grow and form foci, which represents an indirect estimation of neoplastic transformation [24]. As shown in Fig. 6A and B, PC-3 cells treated with **8i** exhibited fewer and smaller colonies compared to the control with a colony formation efficiency of 6% at 2.5  $\mu\text{M}$ , which indicated that compound **8i** could significantly inhibit the proliferation of PC-3 cells in a concentration-dependent manner.

### 2.5. Inhibition of MAPK signaling pathway

Mitogen-activated protein kinase (MAPK) signal transduction pathways are among the most widespread mechanisms of eukaryotic cell regulation and play important roles in cell growth [25]. Some distinct groups of MAPKs have been characterized in mammals: the extracellular signal-regulated kinases (ERK 1/2, ERK3/4, ERK5, ERK 7/8), the Jun *N*-terminal kinases (JNK 1/2/3) and the p38 MAPKs (p38 $\alpha$ / $\beta$ / $\gamma$ / $\delta$ ) [26]. According to the inhibitory results of cells growth, it was hypothesized that **8i** treatment might affect the MAPK signaling pathway of PC-3 cells. To confirm this property, the expression of related MAPK signaling proteins (p-ERK, p-c-Jun, c-Myc, p38, p-p38) were determined. As shown in Fig. 6C and D, the protein levels of p-ERK, p-c-Jun, c-Myc, p38, and p-p38 were decreased in concentration-dependent manners after treatment of compound **8i**. The tests on MAPK signaling pathway illustrated that compound **8i** might inhibit growth of PC-3 cells via inhibiting MAPK signaling pathway.

### 2.6. **8i** induces G1 phase arrest and regulates the expression of G1-related proteins

Targeting the cell cycle of tumor cells has been recognized as a promising strategy for cancer therapy [27]. In this study, compound **8i** was chosen to investigate the effect of our designed derivatives on the cell cycle of PC-3 cells. After treating PC-3 cells with compound **8i** at different concentrations (0  $\mu\text{M}$ , 0.1  $\mu\text{M}$ , 0.5  $\mu\text{M}$ , 2.5  $\mu\text{M}$ ) for 48 h, cells were then fixed and stained with PI for flow cytometry analysis. As shown in Fig. 7, compound **8i** concentration dependently arrested cell cycle at G1 phase, accompanied with the decrease of cells at G2 and S phase. Specifically, the percentage of cells at G1 phase for the high concentration group (2.5  $\mu\text{M}$ ) was 83.32%, about 30% higher than that of the control group.

The G1-phase arrest induced by compound **8i** was further confirmed by investigation of the changes in G1 checkpoint-related proteins, including cyclin D1 and CDK4 [28]. It is well known that the levels of cyclin A and cyclin B1 decreased during G1 phase [29]. Our results as shown in Fig. 7C verified it. Cyclin D-Cdk4 complex accumulation promotes G1-S transition in cell cycle [30]. Compound **8i** down regulated cyclin D1 and CDK4 concentration dependently (Fig. 7C), which lead to cell arrested in G1 phase.

### 2.7. Compound **8i** could not induce apoptosis of PC-3 cells

Based on the biological experiments above, compound **8i** was chosen to perform apoptosis assays to investigate whether **8i** could induce apoptosis of PC-3 cells (Fig. 8A – C). After treatment with different concentrations of compound **8i** (0, 0.1, 0.5 and 2.5  $\mu\text{M}$ ) for 48 h, PC-3 cells were stained with PI and Annexin V-FITC, and then analyzed by the flow cytometry. As illustrated in Fig. 8A and B, the percentage of apoptotic cells was not changed obviously from the control group. Then, we performed to examine the expression of key protein (Bax) related to apoptosis. As shown in Fig. 8C, the expression of Bax protein did not increase after treatment of PC-3 cells with compound **8i**. All these results in Fig. 8 illustrated that compound **8i** could not induce apoptosis of PC-3 cells.

### 2.8. **8i** inhibits migration involved to Wnt signaling pathway on PC-3 cells

From above studies, we can conclude that compound **8i** inhibited growth of PC-3 cells. We next investigated whether compound **8i** could inhibit migration of cancer cells. After incubation at different concentrations (0, 0.1, 0.5, 2.5  $\mu\text{M}$ ) for 48 h, PC-3 cells were stained with crystal violet, and migrated cells were detected and numbered using the high content screening system. As shown in Fig. 9A and B, compound **8i** inhibited migration of PC-3 cells even at low concentration (0.1  $\mu\text{M}$ ). Intriguingly, the inhibition was concentration-independent.

The Wnt signaling pathway plays a critical role in numerous cellular processes including cell proliferation, tissue homeostasis, and cell migration [31–33]. Specifically once activated,  $\beta$ -Catenin disassembles from complex comprised of Axin, APC and GSK3 $\beta$  and translocates into nuclear [34]. Then it interacts with TCF4 which promotes the downstream target gene transcription [35]. According to the transwell migration assay above, we next tested whether compound **8i** could influence Wnt signaling pathway in PC-3 cells. Western blotting analysis of related Wnt pathway proteins ( $\beta$ -catenin, Axin, TCF-4) were performed to confirm this property. As shown in Fig. 9C and D, treatment of PC-3 cells with **8i** resulted in the increase expression of Axin and the decrease expression of  $\beta$ -catenin and TCF-4 in concentration-dependent manners. These results indicated that compound **8i** might inhibit migration of PC-3 cells via Wnt signaling pathway.

## 3. Conclusions

Following our previous work, we designed a series of new formononetin-dithiocarbamate derivatives based on the natural formononetin skeleton by molecular hybridization strategy. All hybrids possessed moderate to good growth inhibition against the tested cancer cells. Particularly, compound **8i** exhibited excellent growth inhibition against PC-3 cells with an

IC<sub>50</sub> value of 1.97 μM. The preliminary SAR illustrated that dithiocarbamate as a reported antitumor scaffold could play potential synergistic effect for natural formononetin skeleton. These hybrids in this work might serve as bioactive fragments and lead compounds for developing more potent cytotoxic agents.

The mechanism investigation showed that compound **8i** inhibited the colony formation, halted cell cycle progression at the G1 phase, altered the expression of cell cycle-related proteins, and induced the inhibition of MAPK signaling pathway. These results investigated that formononetin-dithiocarbamate derivative **8i** could inhibit the growth of PC-3 cells. In addition to the mechanism study, we also explored the effect on migration. **8i** inhibited migration of PC-3 cells in a concentration-dependent manner involved to Wnt signaling pathway. More mechanism studies are underway and will be reported in due course.

## 4. Experimental section

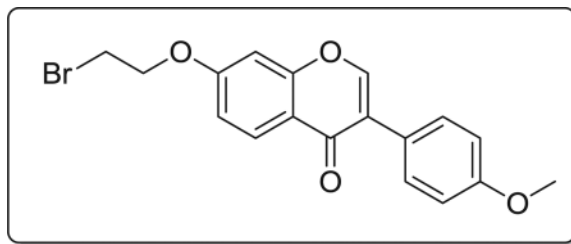
### 4.1. General

Reagents and solvents were used without special treatment. Melting points were determined on an X-5 micromelting apparatus and are uncorrected. <sup>1</sup>H NMR and <sup>13</sup>C NMR spectra were recorded on a Bruker 400 MHz and 100 MHz spectrometer, respectively. High resolution mass spectra (HRMS) of all derivatives were recorded on a Waters Micromass Q-T of Micromass spectrometer by electrospray ionization (ESI).

### 4.2. General procedure for the synthesis of compounds **7a ~ d**

To a solution of formononetin (0.5 mmol, 1.0 eq) in THF (5 mL) was added K<sub>2</sub>CO<sub>3</sub> (0.75 mmol, 1.5 eq) at room temperature, the mixture was stirred for about 30 min, and then the bromide (0.75 mmol, 1.5 eq) was added dropwise. The mixture was stirred at 60 °C. Upon completion, EtOAc and H<sub>2</sub>O were added. The aqueous layer was extracted with EtOAc for several times; the combined organic layers were washed with H<sub>2</sub>O for several times to remove the THF, and then washed with brine, dried over MgSO<sub>4</sub> and evaporated to give the products. The residue was purified with column chromatography (hexane: EtOAc = 6:1) to obtain analogue **7a ~ d**.

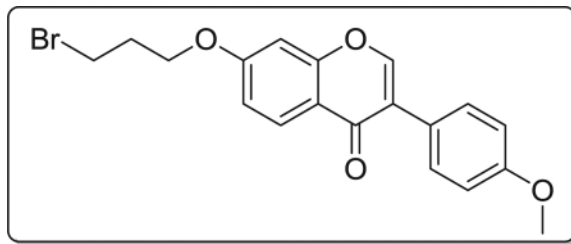
#### 4.2.1. 7-(2-bromoethoxy)-3-(4-methoxyphenyl)-4H-chromen-4-one (**7a**)—



Yield 79%. White solid. Mp: 109–111 °C. <sup>1</sup>H NMR (400 MHz, DMSO) δ 8.50 (s, 1H), 8.12 (d, *J* = 8.9 Hz, 1H), 7.60 (d, *J* = 8.7 Hz, 2H), 7.28 (d, *J* = 2.3 Hz, 1H), 7.19 (dd, *J* = 8.9, 2.3 Hz, 1H), 7.06 (d, *J* = 8.7 Hz, 2H), 4.72–4.43 (m, 2H), 4.02–3.89 (m, 2H), 3.86 (s, 3H). <sup>13</sup>C NMR (100 MHz, DMSO) δ 162.73, 157.82, 154.34, 154.05, 130.45, 127.41, 124.53, 123.81, 118.43, 115.39, 113.95, 109.48, 101.79, 69.01, 55.63, 31.46. HR-MS (ESI): Calcd.

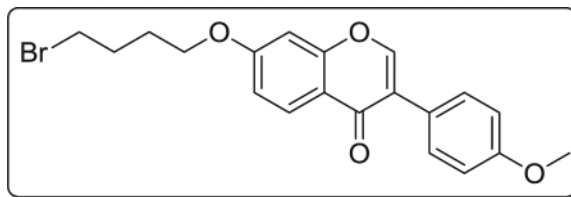
$C_{18}H_{16}BrO_4$ ,  $[M+H]^+$   $m/z$ : 375.0239, found: 375.0232. IR: 3007, 2953, 1609, 1576, 1498, 1446, 544  $cm^{-1}$ .

#### 4.2.2. 7-(3-bromopropoxy)-3-(4-methoxyphenyl)-4H-chromen-4-one (7b)—



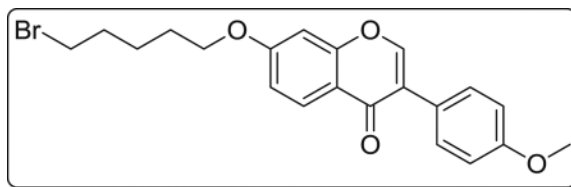
Yield 70%. White solid. Mp: 131–132 °C.  $^1H$  NMR (400 MHz, DMSO)  $\delta$  8.42 (d,  $J$  = 1.2 Hz, 1H), 8.04 (d,  $J$  = 8.9 Hz, 1H), 7.59–7.45 (m, 2H), 7.19 (d,  $J$  = 2.0 Hz, 1H), 7.10 (dd,  $J$  = 8.9, 2.4 Hz, 1H), 7.04–6.89 (m, 2H), 4.25 (t,  $J$  = 6.0 Hz, 2H), 3.79 (s, 3H), 3.70 (t,  $J$  = 6.6 Hz, 2H), 2.31 (p,  $J$  = 6.2 Hz, 2H).  $^{13}C$  NMR (100 MHz, DMSO)  $\delta$  174.59, 162.71, 159.00, 157.37, 153.46, 130.04, 127.01, 124.04, 123.36, 117.71, 114.93, 113.60, 101.17, 66.30, 55.13, 31.56, 30.94. HR-MS (ESI): Calcd.  $C_{19}H_{18}BrO_4$ ,  $[M+H]^+$   $m/z$ : 389.0380, found: 389.0388. IR: 3437, 2930, 1623, 1609, 1513, 1446, 541  $cm^{-1}$ .

#### 4.2.3. 7-(4-bromobutoxy)-3-(4-methoxyphenyl)-4H-chromen-4-one (7c)—



Yield 75%. White solid. Mp: 109–111 °C.  $^1H$  NMR (400 MHz, DMSO)  $\delta$  8.47 (s, 1H), 8.09 (d,  $J$  = 8.9 Hz, 1H), 7.59 (d,  $J$  = 8.7 Hz, 2H), 7.22 (d,  $J$  = 2.2 Hz, 1H), 7.14 (dd,  $J$  = 8.9, 2.2 Hz, 1H), 7.05 (d,  $J$  = 8.7 Hz, 2H), 4.23 (t,  $J$  = 6.2 Hz, 2H), 3.85 (s, 3H), 3.69 (t,  $J$  = 6.5 Hz, 2H), 2.18–2.00 (m, 2H), 2.01–1.80 (m, 2H).  $^{13}C$  NMR (100 MHz, DMSO)  $\delta$  175.11, 163.43, 159.48, 157.90, 153.95, 130.55, 127.43, 124.54, 123.83, 118.03, 115.51, 114.09, 101.54, 68.10, 55.62, 35.23, 29.43, 27.58. HR-MS (ESI): Calcd.  $C_{20}H_{20}BrO_4$ ,  $[M+H]^+$   $m/z$ : 403.0548, found: 403.0545. IR: 2963, 1633, 1608, 1515, 1446, 696  $cm^{-1}$ .

#### 4.2.4. 7-((5-bromopentyl)oxy)-3-(4-methoxyphenyl)-4H-chromen-4-one (7d)—



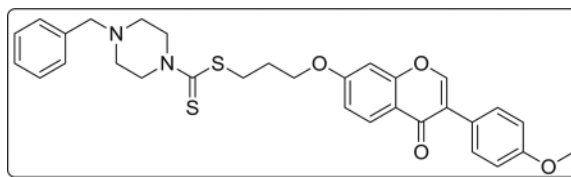
Yield 83%. White solid. Mp: 110–111 °C.  $^1H$  NMR (400 MHz, DMSO)  $\delta$  8.46 (s, 1H), 8.07 (d,  $J$  = 8.9 Hz, 1H), 7.58 (d,  $J$  = 8.7 Hz, 2H), 7.19 (d,  $J$  = 2.2 Hz, 1H), 7.12 (dd,  $J$  = 8.9, 2.3 Hz, 1H), 7.04 (d,  $J$  = 8.8 Hz, 2H), 4.18 (t,  $J$  = 6.4 Hz, 2H), 3.84 (s, 3H), 3.62 (t,  $J$  = 6.7 Hz, 2H), 2.03–1.89 (m, 2H), 1.89–1.79 (m, 2H), 1.61 (dt,  $J$  = 15.1, 7.6 Hz, 2H).  $^{13}C$  NMR (100

MHz, DMSO)  $\delta$  175.10, 163.52, 159.47, 157.90, 153.91, 130.53, 127.40, 124.55, 123.82, 117.98, 115.50, 114.08, 101.47, 68.79, 55.62, 35.51, 32.37, 28.00, 24.68. HR-MS (ESI): Calcd.  $C_{21}H_{22}BrO_4$ ,  $[M+H]^+ m/z$ : 417.0707, found: 417.0701. IR: 3450, 2962, 1632, 1610, 1576, 1515, 1446, 542  $cm^{-1}$ .

### 4.3. General procedure for the synthesis of compounds 8a ~ j

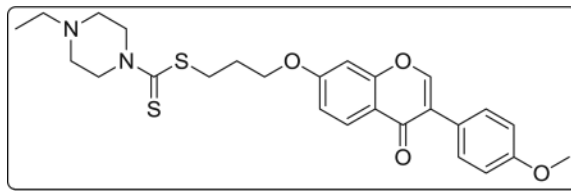
$CS_2$  (2 eq) was added to the mixture of substituted amine (0.1 g, 1 eq) and  $Na_3PO_4 \cdot 12H_2O$  (0.5 eq) in acetone (5 mL). The mixture was stirred at room temperature for 0.5 h. Then product 7a ~ d (1 eq) was added to the mixture cautiously, the mixture was continued to stir at room temperature for another 0.5 h. Upon completion, the solvent was removed under reduced pressure, the residue was extracted with dichloromethane, washed with water, brine, dried with anhydrous  $Na_2SO_4$  and concentrated under reduced pressure. The residue was purified with column chromatography (hexane: EtOAc = 7:1) to obtain analogue 8a ~ j.

#### 4.3.1. 3-((3-(4-methoxyphenyl)-4-oxo-4H-chromen-7-yl)oxy) propyl 4-benzylpiperazine-1-carbodithioate (8a)—



Yield 83%. White solid. Mp: 124–125 °C.  $^1H$  NMR (400 MHz, DMSO)  $\delta$  8.42 (s, 1H), 8.03 (d,  $J$  = 8.9 Hz, 1H), 7.53 (d,  $J$  = 8.7 Hz, 2H), 7.38–7.29 (m, 4H), 7.29–7.22 (m, 1H), 7.17 (d,  $J$  = 2.2 Hz, 1H), 7.09 (dd,  $J$  = 8.9, 2.3 Hz, 1H), 7.00 (d,  $J$  = 8.8 Hz, 2H), 4.22 (t,  $J$  = 6.1 Hz, 4H), 3.92 (s, 2H), 3.79 (s, 3H), 3.51 (s, 2H), 3.42 (t,  $J$  = 7.2 Hz, 2H), 2.45 (s, 4H), 2.22–2.09 (m, 2H).  $^{13}C$  NMR (100 MHz, DMSO)  $\delta$  194.74, 174.60, 162.81, 158.99, 157.38, 153.45, 137.53, 130.04, 128.91, 128.22, 127.09, 126.96, 124.05, 123.35, 117.63, 115.02, 113.60, 101.12, 67.14, 61.27, 55.13, 51.93, 32.72, 27.86. HR-MS (ESI): Calcd.  $C_{31}H_{33}N_2O_4S_2$ ,  $[M+H]^+ m/z$ : 561.1885, found: 561.1882. IR: 3445, 2935, 1628, 1609, 1566, 1514, 1445, 1251  $cm^{-1}$ .

#### 4.3.2. 3-((3-(4-methoxyphenyl)-4-oxo-4H-chromen-7-yl)oxy) propyl 4-ethylpiperazine-1-carbodithioate (8b)—

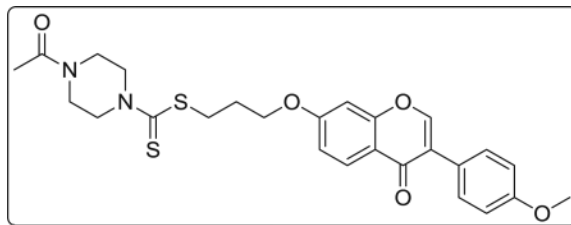


Yield 85%. Yellow solid. Mp: 167–168 °C.  $^1H$  NMR (400 MHz, DMSO)  $\delta$  8.43 (s, 1H), 8.03 (d,  $J$  = 8.9 Hz, 1H), 7.53 (d,  $J$  = 8.8 Hz, 2H), 7.18 (d,  $J$  = 2.3 Hz, 1H), 7.09 (dd,  $J$  = 8.9, 2.3 Hz, 1H), 7.00 (d,  $J$  = 8.8 Hz, 2H), 4.22 (t,  $J$  = 6.1 Hz, 4H), 3.91 (s, 2H), 3.79 (s, 3H), 3.42 (t,  $J$  = 7.2 Hz, 2H), 2.47–2.39 (m, 4H), 2.36 (q,  $J$  = 7.2 Hz, 2H), 2.21–2.10 (m, 2H), 1.01 (t,  $J$  = 7.2 Hz, 3H).  $^{13}C$  NMR (100 MHz, DMSO)  $\delta$  194.69, 174.60, 162.82, 158.99,



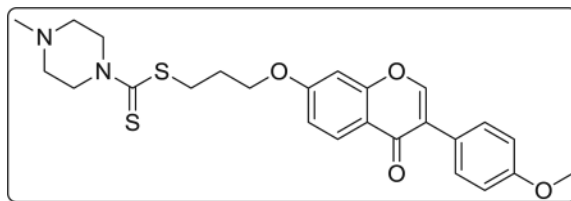
157.38, 153.46, 130.05, 126.96, 124.05, 123.35, 117.62, 115.03, 113.61, 101.13, 67.15, 55.14, 51.71, 50.99, 32.69, 27.87, 11.85. HR-MS (ESI): Calcd.  $C_{26}H_{31}N_2O_4S_2$ ,  $[M+H]^+ m/z$ : 499.1729, found: 499.1725. IR: 3423, 2969, 1625, 1594, 1576, 1513, 1467, 1253, 1181, 1031  $cm^{-1}$ .

**4.3.3. 3-((3-(4-methoxyphenyl)-4-oxo-4H-chromen-7-yl)oxy) propyl 4-acetylpiperazine-1-carbodithioate (8c)—**



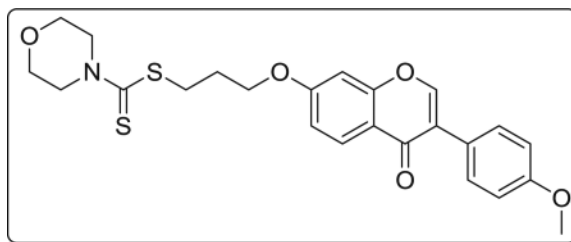
Yield 78%. White solid. Mp: 174–176 °C.  $^1H$  NMR (400 MHz, DMSO)  $\delta$  8.43 (s, 1H), 8.04 (d,  $J = 8.9$  Hz, 1H), 7.53 (d,  $J = 8.7$  Hz, 2H), 7.18 (d,  $J = 2.2$  Hz, 1H), 7.10 (dd,  $J = 8.9, 2.3$  Hz, 1H), 7.00 (d,  $J = 8.8$  Hz, 2H), 4.23 (t,  $J = 6.1$  Hz, 4H), 3.97 (s, 2H), 3.79 (s, 3H), 3.64–3.55 (m, 4H), 3.44 (t,  $J = 7.2$  Hz, 2H), 2.24–2.11 (m, 2H), 2.03 (s, 3H).  $^{13}C$  NMR (100 MHz, DMSO)  $\delta$  195.33, 174.61, 168.68, 162.81, 158.99, 157.38, 153.47, 130.05, 126.97, 124.04, 123.35, 117.62, 115.05, 113.61, 101.13, 67.15, 55.15, 44.41, 32.69, 27.81, 21.21. HR-MS (ESI): Calcd.  $C_{26}H_{29}N_2O_5S_2$ ,  $[M+H]^+ m/z$ : 513.1510, found: 513.1518. IR: 3439, 2922, 1648, 1633, 1609, 1567, 1515, 1444, 1252, 1026  $cm^{-1}$ .

**4.3.4. 3-((3-(4-methoxyphenyl)-4-oxo-4H-chromen-7-yl)oxy) propyl 4-methylpiperazine-1-carbodithioate (8d)—**



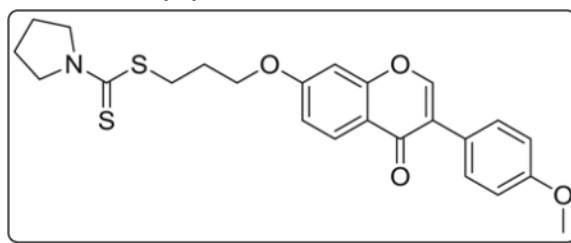
Yield 82%. Yellow solid. Mp: 167–169 °C.  $^1H$  NMR (400 MHz, DMSO)  $\delta$  8.43 (s, 1H), 8.04 (d,  $J = 8.9$  Hz, 1H), 7.53 (d,  $J = 8.7$  Hz, 2H), 7.18 (d,  $J = 2.3$  Hz, 1H), 7.10 (dd,  $J = 8.9, 2.3$  Hz, 1H), 7.00 (d,  $J = 8.8$  Hz, 2H), 4.22 (t,  $J = 6.1$  Hz, 4H), 3.92 (s, 2H), 3.79 (s, 3H), 3.42 (t,  $J = 7.2$  Hz, 2H), 2.44–2.32 (m, 4H), 2.20 (s, 3H), 2.14 (dd,  $J = 13.7, 7.0$  Hz, 2H).  $^{13}C$  NMR (100 MHz, DMSO)  $\delta$  194.86, 174.60, 162.81, 158.99, 157.38, 153.47, 130.04, 126.96, 124.04, 123.35, 117.62, 115.03, 113.60, 101.12, 67.15, 55.13, 53.94, 45.03, 32.71, 27.86. HR-MS (ESI): Calcd.  $C_{25}H_{29}N_2O_4S_2$ ,  $[M+H]^+ m/z$ : 485.1574, found: 485.1569. IR: 3442, 2940, 1625, 1595, 1576, 1513, 1442, 1294, 1249, 1198, 1181, 1031  $cm^{-1}$ .

**4.3.5. 3-((3-(4-methoxyphenyl)-4-oxo-4H-chromen-7-yl)oxy) propyl morpholine-4-carbodithioate (8e)—**



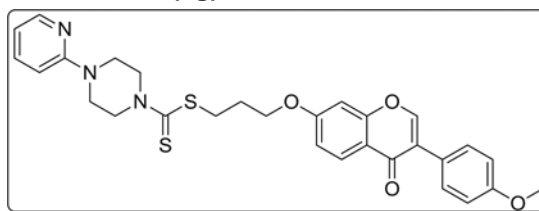
Yield 79%. White solid. Mp: 156–158 °C.  $^1\text{H}$  NMR (400 MHz, DMSO)  $\delta$  8.43 (s, 1H), 8.04 (d,  $J$  = 8.9 Hz, 1H), 7.53 (d,  $J$  = 8.8 Hz, 2H), 7.18 (d,  $J$  = 2.3 Hz, 1H), 7.10 (dd,  $J$  = 8.9, 2.3 Hz, 1H), 7.00 (d,  $J$  = 8.8 Hz, 2H), 4.23 (t,  $J$  = 6.1 Hz, 4H), 3.94 (s, 2H), 3.79 (s, 3H), 3.72–3.60 (m, 4H), 3.44 (t,  $J$  = 7.2 Hz, 2H), 2.23–2.11 (m, 2H).  $^{13}\text{C}$  NMR (100 MHz, DMSO)  $\delta$  195.39, 174.60, 162.81, 158.99, 157.38, 153.47, 130.05, 126.97, 124.04, 123.35, 117.62, 115.03, 113.60, 101.12, 67.14, 65.56, 55.13, 32.56, 27.84. HR-MS (ESI): Calcd.  $\text{C}_{24}\text{H}_{26}\text{NO}_5\text{S}_2$ ,  $[\text{M}+\text{H}]^+ m/z$ : 472.1257, found: 472.1252. IR: 3442, 3077, 1638, 1624, 1609, 1575, 1514, 1441, 1250, 1199, 1177, 1138, 1116  $\text{cm}^{-1}$ .

#### 4.3.6. 3-((3-(4-methoxyphenyl)-4-oxo-4H-chromen-7-yl)oxy) propyl pyrrolidine-1-carbodithioate (8f)—



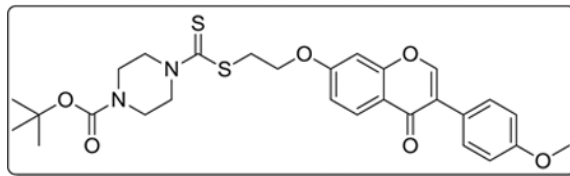
Yield 81%. White solid. Mp: 159–161 °C.  $^1\text{H}$  NMR (400 MHz, DMSO)  $\delta$  8.43 (s, 1H), 8.04 (d,  $J$  = 8.9 Hz, 1H), 7.53 (d,  $J$  = 8.8 Hz, 2H), 7.18 (d,  $J$  = 2.3 Hz, 1H), 7.09 (dd,  $J$  = 8.9, 2.3 Hz, 1H), 7.00 (d,  $J$  = 8.8 Hz, 2H), 4.22 (t,  $J$  = 6.2 Hz, 2H), 3.79 (s, 3H), 3.76 (d,  $J$  = 6.9 Hz, 2H), 3.62 (t,  $J$  = 6.8 Hz, 2H), 3.40 (t,  $J$  = 7.2 Hz, 2H), 2.23–2.10 (m, 2H), 2.07–1.96 (m, 2H), 1.91 (p,  $J$  = 6.7 Hz, 2H).  $^{13}\text{C}$  NMR (100 MHz, DMSO)  $\delta$  190.61, 174.60, 162.83, 158.99, 157.39, 153.47, 130.05, 126.96, 124.05, 123.35, 117.62, 115.04, 113.60, 101.11, 67.15, 55.13, 54.93, 50.53, 32.03, 28.03, 25.53, 23.71. HR-MS (ESI): Calcd.  $\text{C}_{24}\text{H}_{26}\text{NO}_4\text{S}_2$ ,  $[\text{M}+\text{H}]^+ m/z$ : 456.1306, found: 456.1303. IR: 3445, 2848, 1623, 1609, 1574, 1513, 1443, 1290, 1265, 1201, 1177, 1031  $\text{cm}^{-1}$ .

#### 4.3.7. 3-((3-(4-methoxyphenyl)-4-oxo-4H-chromen-7-yl)oxy) propyl 4-(pyridin-2-yl)piperazine-1-carbodithioate (8g)—



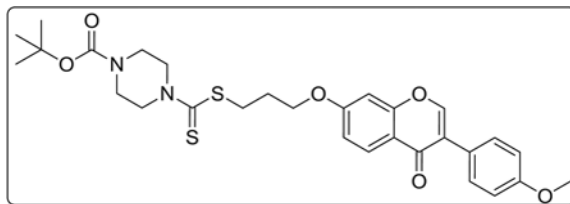
Yield 84%. White solid. Mp: 178–180 °C.  $^1\text{H}$  NMR (400 MHz, DMSO)  $\delta$  8.42 (s, 1H), 8.13 (dd,  $J = 4.9, 1.3$  Hz, 1H), 8.04 (d,  $J = 8.9$  Hz, 1H), 7.60–7.55 (m, 1H), 7.55–7.48 (m, 2H), 7.19 (d,  $J = 2.3$  Hz, 1H), 7.10 (dd,  $J = 8.9, 2.3$  Hz, 1H), 7.00 (d,  $J = 8.8$  Hz, 2H), 6.81 (d,  $J = 8.6$  Hz, 1H), 6.68 (dd,  $J = 7.0, 5.0$  Hz, 1H), 4.34 (s, 2H), 4.24 (t,  $J = 6.1$  Hz, 2H), 4.06 (s, 2H), 3.79 (s, 3H), 3.66 (s, 4H), 3.46 (t,  $J = 7.1$  Hz, 2H), 2.26–2.08 (m, 2H).  $^{13}\text{C}$  NMR (100 MHz, DMSO)  $\delta$  194.93, 174.52, 162.74, 158.91, 158.07, 157.30, 153.38, 147.47, 137.58, 129.97, 126.88, 124.42, 123.27, 117.54, 114.97, 113.52, 113.18, 106.86, 101.04, 67.07, 55.05, 43.51, 32.57, 27.76. HR-MS (ESI): Calcd.  $\text{C}_{29}\text{H}_{30}\text{N}_3\text{O}_4\text{S}_2$ ,  $[\text{M}+\text{H}]^+ m/z$ : 548.1684, found: 548.1678. IR: 3441, 2915, 1639, 1627, 1599, 1567, 1514, 1442, 1251, 1224, 1035  $\text{cm}^{-1}$ .

**4.3.8. tert-butyl 4-(((2-((3-(4-methoxyphenyl)-4-oxo-4H-chromen-7-yl)oxy)ethyl)thio)carbonothioyl)piperazine-1-carboxylate (8h)—**



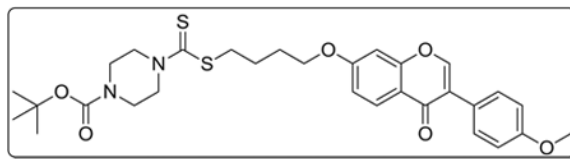
Yield 79%. White solid. Mp: 140–142 °C.  $^1\text{H}$  NMR (400 MHz, DMSO)  $\delta$  8.43 (s, 1H), 8.04 (d,  $J = 8.9$  Hz, 1H), 7.53 (d,  $J = 8.6$  Hz, 2H), 7.26 (d,  $J = 1.8$  Hz, 1H), 7.11 (dd,  $J = 9.0, 2.0$  Hz, 1H), 7.00 (d,  $J = 8.6$  Hz, 2H), 4.38 (t,  $J = 6.2$  Hz, 2H), 4.26 (s, 2H), 3.97 (s, 2H), 3.80 (s, 3H), 3.77 (t,  $J = 6.2$  Hz, 2H), 3.48 (s, 4H), 1.42 (s, 9H).  $^{13}\text{C}$  NMR (100 MHz, DMSO)  $\delta$  195.25, 190.44, 175.10, 162.88, 159.52, 157.85, 154.03, 130.55, 127.56, 124.33, 123.87, 118.19, 115.46, 114.10, 101.78, 79.89, 75.53, 67.15, 55.63, 35.36, 28.49. HR-MS (ESI): Calcd.  $\text{C}_{28}\text{H}_{33}\text{N}_2\text{O}_6\text{S}_2$ ,  $[\text{M}+\text{H}]^+ m/z$ : 557.1788, found: 557.1780. IR: 3440, 2972, 1701, 1627, 1513, 1443, 1289, 1251, 1179  $\text{cm}^{-1}$ .

**4.3.9. tert-butyl 4-(((3-((3-(4-methoxyphenyl)-4-oxo-4H-chromen-7-yl)oxy)propyl)thio)carbonothioyl)piperazine-1-carboxylate (8i)—**



Yield 83%. White solid. Mp: 165–167 °C.  $^1\text{H}$  NMR (400 MHz, DMSO)  $\delta$  8.42 (s, 1H), 8.03 (d,  $J = 8.9$  Hz, 1H), 7.53 (d,  $J = 8.8$  Hz, 2H), 7.17 (d,  $J = 2.3$  Hz, 1H), 7.09 (dd,  $J = 8.9, 2.3$  Hz, 1H), 7.00 (d,  $J = 8.8$  Hz, 2H), 4.22 (t,  $J = 6.1$  Hz, 4H), 3.95 (s, 2H), 3.79 (s, 3H), 3.44 (dd,  $J = 15.1, 7.3$  Hz, 6H), 2.22–2.10 (m, 2H), 1.42 (s, 9H).  $^{13}\text{C}$  NMR (100 MHz, DMSO)  $\delta$  195.33, 174.59, 162.80, 158.98, 157.37, 153.68, 153.44, 130.04, 126.95, 124.04, 123.34, 117.62, 115.02, 113.59, 101.10, 79.35, 67.14, 55.13, 32.69, 27.99, 27.81, 18.53. HR-MS (ESI): Calcd.  $\text{C}_{29}\text{H}_{35}\text{N}_2\text{O}_6\text{S}_2$ ,  $[\text{M}+\text{H}]^+ m/z$ : 571.1940, found: 571.1937. IR: 3440, 2931, 1690, 1608, 1566, 1513, 1444, 1419, 1250, 1223, 1178 1031  $\text{cm}^{-1}$ .

#### 4.3.10. tert-butyl 4-(((4-((3-(4-methoxyphenyl)-4-oxo-4H-chromen-7-yl)oxy)butyl)thio)carbonothioyl)piperazine-1-carboxylate (**8j**)—



Yield 85%. White solid. Mp: 143–144 °C. <sup>1</sup>H NMR (400 MHz, DMSO) δ 8.41 (s, 1H), 8.02 (d, *J* = 8.9 Hz, 1H), 7.53 (d, *J* = 8.7 Hz, 2H), 7.15 (d, *J* = 2.2 Hz, 1H), 7.07 (dd, *J* = 8.9, 2.2 Hz, 1H), 7.00 (d, *J* = 8.8 Hz, 2H), 4.23 (s, 2H), 4.16 (t, *J* = 5.8 Hz, 2H), 3.94 (s, 2H), 3.51–3.42 (m, 4H), 1.95–1.76 (m, 4H), 1.42 (s, 9H). <sup>13</sup>C NMR (100 MHz, DMSO) δ 196.13, 175.10, 163.47, 159.48, 157.89, 154.18, 153.92, 130.54, 127.41, 124.55, 123.83, 118.01, 115.51, 114.09, 101.51, 79.86, 68.48, 55.62, 36.24, 28.49, 28.09, 25.55. HR-MS (ESI): Calcd. C<sub>30</sub>H<sub>37</sub>N<sub>2</sub>O<sub>6</sub>S<sub>2</sub>, [M+H]<sup>+</sup> *m/z*: 585.2096, found: 585.2093. IR: 3435, 2931, 1707, 1630, 1514, 1445, 1406, 1252, 1264, 1168 1027 cm<sup>-1</sup>.

#### 4.4. Antiproliferative activity assays

MGC-803 cells (human gastric cancer), EC-109 (human esophagus cancer), PC-3 (human prostate Cancer) and GES-1 (human gastric epithelial cell) were cultured by RPMI 1640 medium with 10% FBS and 100 U/ml penicillin and 0.1 mg/ml streptomycin in the 37 °C in an atmosphere containing 5% CO<sub>2</sub>. After 24 h of incubation, the culture medium was removed and fresh medium containing various concentrations of the candidate compounds was added to each well [23]. The cells were then incubated for 48 h, MTT assays were performed and cell viability was assessed at 570 nm by a microplate reader (Biotech, China). All experiments were performed three times.

#### 4.5. Clonogenicity assay

PC-3 cells were seeded in a 6-well plate and incubated for 24 h, then the media were replaced with fresh media containing different concentrations of compound **8i**. After a week of treatment, the cells were washed twice with PBS, fixed with 4% paraformaldehyde, and colonies were visualized using 0.1% crystal violet staining. The cells were imaged, and the number of colonies were quantified by Image J software (Developed by National Institutes of Health).

#### 4.6. Cell cycle distribution assay

Cells were seeded in 6-well plates and treated with 0, 0.1, 0.5 and 2.5 μM of compound **8i** for 48 h. Then cells were collected and fixed by 70% ethanol at 4 °C overnight. The fixed cells were washed with PBS and resuspended in 100 μl PBS containing 10 mg/mL RNaseA and 50 mg/mL PI for 20 min in dark. Samples were then analyzed for DNA content by flow cytometry (Becton, Dickinson and Company, NJ.).

#### 4.7. Cell apoptosis assay

Cells were seeded in 6-well plates and treated with 0, 0.1, 0.5 and 2.5 μM of **8i** for 48 h. Then the cells were collected and suspended in binding buffer containing Annexin V-FITC

(0.5 mg/mL) and PI (0.5 mg/mL) and incubated in dark for 20 min and analyzed by flow cytometry (Becton, Dickinson and Company, NJ).

#### 4.8. Transwell migration assay

100 mL medium containing 1% FBS, different concentrations (0, 0.1, 0.5 and 2.5  $\mu\text{M}$ ) of compound **8i** and  $10^4$  cells were added to each upper chamber. In the lower chamber, 510 mL medium with 20% FBS was used as chemoattractant. After incubation for 48 h, both chambers were washed by PBS for three times. After staining with Hoechst 33258 (10 mg/mL) and twice wash, high content screening system (ArrayScan XTI, Thermo Fisher Scientific, MA) was used to detect and number migrated cells.

#### 4.9. Western blot analysis

PC-3 cells were treated with different concentrations (0, 0.1, 0.5 and 2.5  $\mu\text{M}$ ) of compound **8i** for 48 h, the cells were collected, lysed in RIPA buffer contained a protease inhibitor cocktail for 30 min, followed by centrifugation at  $1.2 \times 10^4$  rpm for 30 min at 4 °C. After the collection of supernatant, the protein concentration was detected using a micro-BCA protein assay kit. The total protein extracts were boiled with 5  $\times$  loading buffer, separated by SDS-PAGE and transferred to nitrocellulose membrane. The membranes were blocked with 5% skim milk at room temperature for 2 h, and then incubated overnight at 4 °C with primary antibodies. After washing the membrane with the secondary antibody (1:5000) at room temperature for 2 h. Finally, the blots were washed in TBST/TBS. The detection of specific proteins was carried out with an ECL western blotting kit.

#### 4.10. Statistical analysis

Data are presented as mean  $\pm$  SD from three independent experiments. SPSS version 10.0 (SPSS, Inc., Chicago, IL, USA) was used to calculate  $\text{IC}_{50}$  values and one-way analysis of variance (ANOVA). \* $P < 0.05$  and \*\* $P < 0.01$  were considered to indicate as statistical significant difference.

### Supplementary Material

Refer to Web version on PubMed Central for supplementary material.

### Acknowledgments

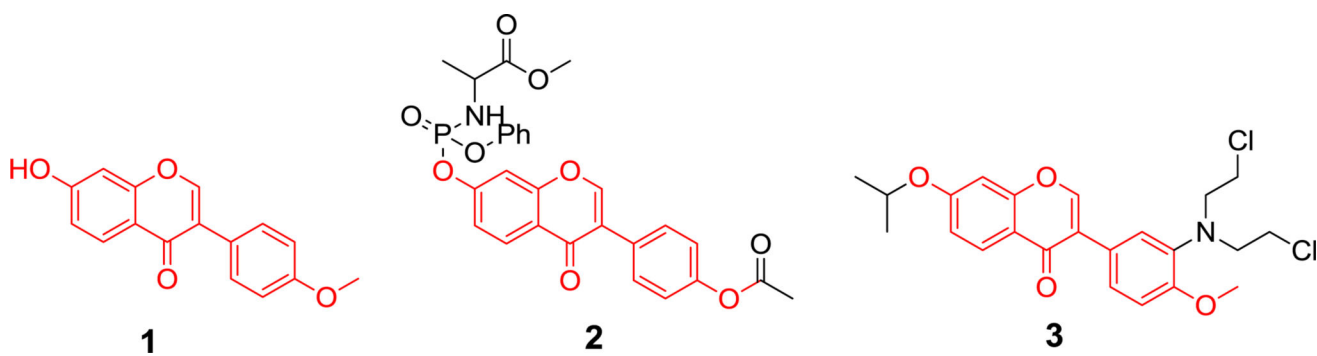
This work was supported by the National Natural Sciences Foundations of China (No. 81673322, 81273393, 81430085, 21372206, and 81172937), Ph.D. Educational Award from Ministry of Education (No. 20134101130001).

### References

1. Cragg GM, Newman DJ. Natural products: a continuing source of novel drug leads. *Biochim. Biophys. Acta.* 2013; 1830:3670–3695. [PubMed: 23428572]
2. Mu H, Bai YH, Wang ST, Zhu ZM, Zhang YW. Research on antioxidant effects and estrogenic effect of formononetin from *Trifolium pratense* (red clover). *Phytomedicine.* 2009; 16:314–319. [PubMed: 18757188]

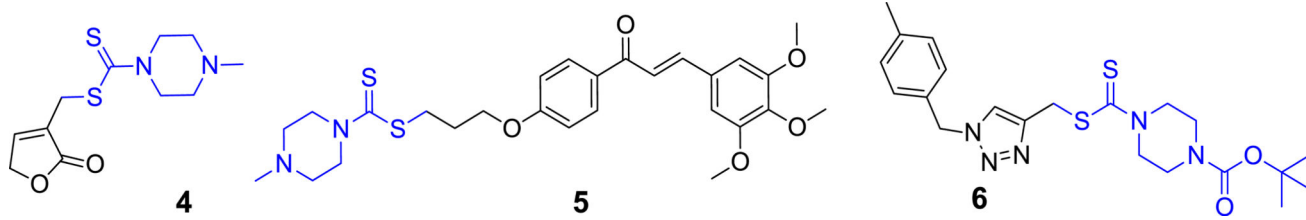
3. Li T, Zhao X, Mo Z, Huang W, Yan H, Ling Z, Ye Y. Formononetin promotes cell cycle arrest via downregulation of Akt/Cyclin D1/CDK4 in human prostate cancer cells. *Cell. Physiol. Biochem.* 2014; 34:1351–1358. [PubMed: 25301361]
4. Sun T, Liu R, Cao Y-x. Vasorelaxant and antihypertensive effects of formononetin through endothelium-dependent and -independent mechanisms. *Acta Pharmacol. Sin.* 2011; 32:1009–1018. [PubMed: 21818108]
5. Gafner S, Bergeron C, Villinski JR, Godejohann M, Kessler P, Cardellina JH, Ferreira D, Feghali K, Grenier D. Isoflavonoids and coumarins from glycyrrhiza uralensis: antibacterial activity against oral pathogens and conversion of Isoflavans into Isoflavan-Quinones during purification. *J. Nat. Prod.* 2011; 74:2514–2519. [PubMed: 22074222]
6. Wu XY, Xu H, Wu ZF, Chen C, Liu JY, Wu GN, Yao XQ, Liu FK, Li G, Shen L. Formononetin, a novel FGFR2 inhibitor, potently inhibits angiogenesis and tumor growth in preclinical models. *Oncotarget.* 2015; 6:44563–44578. [PubMed: 26575424]
7. Coward L, Barnes NC, Setchell KDR, Barnes S. Genistein, daidzein, and their beta.-glycoside conjugates: antitumor isoflavones in soybean foods from American and Asian diets. *J. Agric. Food Chem.* 1993; 41:1961–1967.
8. Choi CW, Choi YH, Cha M-R, Kim YS, Yon Gh, Kim Y-K, Choi SU, Kim YH, Ryu SY. Antitumor components isolated from the heartwood extract of *Dalbergia odorifera*. *J. Korean Soc. Appl. Biol. Chem.* 2009; 52:375–379.
9. Novak EM, Silva MSeC, Marcucci MC, Sawaya ACHF, Gimenez-Cassina Lopez B, Fortes MAHZ, Giorgi RR, Marumo KT, Rodrigues RF, Maria DA. Antitumoural activity of Brazilian red propolis fraction enriched with xanthochymol and formononetin: an in vitro and in vivo study. *J. Funct. Foods.* 2014; 11:91–102.
10. Li, Y-q, Yang, F., Wang, L., Cao, Z., Han, T-j, Duan, Z-a, Li, Z., Zhao, W-j. Phosphoramidate protides of five flavones and their antiproliferative activity against HepG2 and L-O2 cell lines. *Eur. J. Med. Chem.* 2016; 112:196–208. [PubMed: 26896708]
11. Ren J, Xu H-J, Cheng H, Xin W-Q, Chen X, K Hu. Synthesis and antitumor activity of formononetin nitrogen mustard derivatives. *Eur. J. Med. Chem.* 2012; 54:175–187. [PubMed: 22633834]
12. Len C, Boulogne-Merlot A-S, Postel D, Ronco G, Villa P, Goubert C, Jeufrault E, Mathon B, Simon H. Synthesis and antifungal activity of novel bis(dithiocarbamate) derivatives of glycerol. *J. Agric. Food Chem.* 1996; 44:2856–2858.
13. Manav N, Mishra AK, Kaushik NK. In vitro antitumour and antibacterial studies of some Pt(IV) dithiocarbamate complexes. *Spectrochim. Acta Part A Mol. Biomol. Spectrosc.* 2006; 65:32–35.
14. Innocenti A, Scozzafava A, Supuran CT. Carbonic anhydrase inhibitors. Inhibition of transmembrane isoforms IX, XII, and XIV with less investigated anions including trithiocarbonate and dithiocarbamate. *Bioorg. Med. Chem. Lett.* 2010; 20:1548–1550. [PubMed: 20137947]
15. Li R-D, Wang H-L, Li Y-B, Wang Z-Q, Wang X, Wang Y-T, Ge Z-M, Li R-T. Discovery and optimization of novel dual dithiocarbamates as potent anticancer agents. *Eur. J. Med. Chem.* 2015; 93:381–391. [PubMed: 25725374]
16. Altıntop MD, Sever B, Akalın Çiftçi G, Kucukoglu K, Özdemir A, Soleimani SS, Nadaroglu H, Kaplancıklı ZA. Synthesis and evaluation of new benzodioxole-based dithiocarbamate derivatives as potential anticancer agents and hCA-I and hCA-II inhibitors. *Eur. J. Med. Chem.* 2017; 125:190–196. [PubMed: 27657811]
17. Bozdag M, Carta F, Vullo D, Akdemir A, Isik S, Lanzi C, Scozzafava A, Masini E, Supuran CT. Synthesis of a new series of dithiocarbamates with effective human carbonic anhydrase inhibitory activity and antiglaucoma action. *Bioorg. Med. Chem.* 2015; 23:2368–2376. [PubMed: 25846066]
18. Wang X-J, Xu H-W, Guo L-L, Zheng J-X, Xu B, Guo X, Zheng C-X, Liu H-M. Synthesis and in vitro antitumor activity of new butenolide-containing dithiocarbamates. *Bioorg. Med. Chem. Lett.* 2011; 21:3074–3077. [PubMed: 21486694]
19. Fu D-J, Zhang S-Y, Liu Y-C, Zhang L, Liu J-J, Song J, Zhao R-H, Li F, Sun H-H, Liu H-M, Zhang Y-B. Design, synthesis and antiproliferative activity studies of novel dithiocarbamate-chalcone derivatives. *Bioorg. Med. Chem. Lett.* 2016; 26:3918–3922. [PubMed: 27423479]

20. Zheng Y-C, Duan Y-C, Ma J-L, Xu R-M, Zi X, Lv W-L, Wang M-M, Ye X-W, Zhu S, Mobley D, Zhu Y-Y, Wang J-W, Li J-F, Wang Z-R, Zhao W, Liu H-M. Triazole–dithiocarbamate based selective lysine specific demethylase 1 (LSD1) inactivators inhibit gastric cancer cell growth, invasion, and migration. *J. Med. Chem.* 2013; 56:8543–8560. [PubMed: 24131029]
21. Fu D-J, Zhang S-Y, Liu Y-C, Yue X-X, Liu J-J, Song J, Zhao R-H, Li F, Sun H-H, Zhang Y-B, Liu H-M. Design, synthesis and antiproliferative activity studies of 1,2,3-triazole- chalcones. *MedChemComm.* 2016; 7:1664–1671.
22. Duan Y-C, Zheng Y-C, Li X-C, Wang M-M, Ye X-W, Guan Y-Y, Liu G-Z, Zheng J-X, Liu H-M. Design, synthesis and antiproliferative activity studies of novel 1,2,3-triazole-dithiocarbamate-urea hybrids. *Eur. J. Med. Chem.* 2013; 64:99–110. [PubMed: 23644193]
23. Duan Y-C, Ma Y-C, Zhang E, Shi X-J, Wang M-M, Ye X-W, Liu H-M. Design and synthesis of novel 1,2,3-triazole-dithiocarbamate hybrids as potential anticancer agents. *Eur. J. Med. Chem.* 2013; 62:11–19. [PubMed: 23353743]
24. Wang C, Jiang L, Wang S, Shi H, Wang J, Wang R, Li Y, Dou Y, Liu Y, Hou G, Ke Y, Liu H. The antitumor activity of the novel compound jesridonin on human esophageal carcinoma cells. *PLoS One.* 2015; 10:e0130284. [PubMed: 26103161]
25. Kyriakis JM, Avruch J. Mammalian mitogen-activated protein kinase signal transduction pathways activated by stress and inflammation. *Physiol. Rev.* 2001; 81:807–869. [PubMed: 11274345]
26. Kyriakis JM, Avruch J. Mammalian MAPK signal transduction pathways activated by stress and inflammation: a 10-year update. *Physiol. Rev.* 2012; 92:689. [PubMed: 22535895]
27. Schwartz GK, Shah MA. Targeting the cell cycle: a new approach to cancer therapy. *J. Clin. Oncol.* 2005; 23:9408–9421. [PubMed: 16361640]
28. Islam MS, Park S, Song C, Kadi AA, Kwon Y, Rahman AFMM. Fluorescein hydrazones: a series of novel non-intercalative topoisomerase II $\alpha$  catalytic inhibitors induce G1 arrest and apoptosis in breast and colon cancer cells. *Eur. J. Med. Chem.* 2017; 125:49–67. [PubMed: 27654394]
29. Matsushime H, Roussel MF, Ashmun RA, Sherr CJ. Colony-stimulating factor 1 regulates novel cyclins during the G1 phase of the cell cycle. *Cell.* 1991; 65:701–713. [PubMed: 1827757]
30. Tiwari S, Roel C, Wills R, Casinelli G, Tanwir M, Takane KK, Fiaschi-Taesch NM. Early and late G1/S cyclins and Cdks act complementarily to enhance authentic human  $\beta$ -Cell proliferation and expansion. *Diabetes.* 2015; 64:3485–3498. [PubMed: 26159177]
31. Bienz M, Clevers H. Linking colorectal cancer to Wnt signaling. *Cell.* 2000; 103:311–320. [PubMed: 11057903]
32. Nusse R. Wnt signaling in disease and in development. *Cell Res.* 2005; 15:28–32. [PubMed: 15686623]
33. Veeman MT, Axelrod JD, Moon RT. A second canon: functions and mechanisms of  $\beta$ -catenin-independent Wnt signaling. *Dev. Cell.* 2003; 5:367–377. [PubMed: 12967557]
34. Stamos JL, Weis WI. The  $\beta$ -catenin destruction complex, cold spring harb. *Perspect. Biol.* 2013; 5:a007898.
35. Yu Y, Wu J, Wang Y, Zhao T, Ma B, Liu Y, Fang W, Zhu W-G, Zhang H. Kindlin 2 forms a transcriptional complex with  $\beta$ -catenin and TCF4 to enhance Wnt signalling. *EMBO Rep.* 2012; 13:750–758. [PubMed: 22699938]

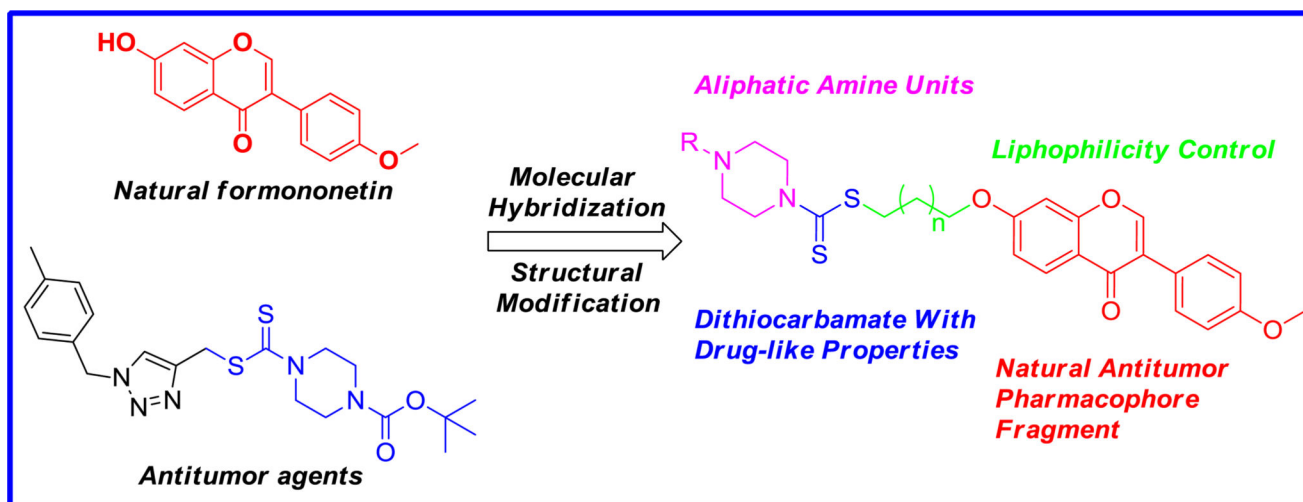


**Fig. 1.**  
Formononetin derivatives with anticancer activity.

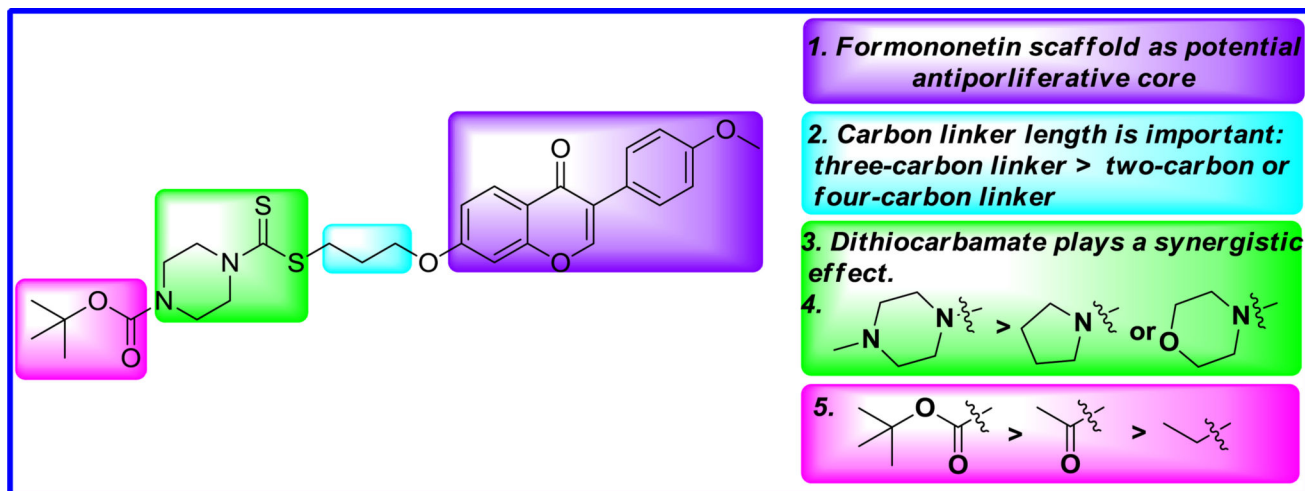




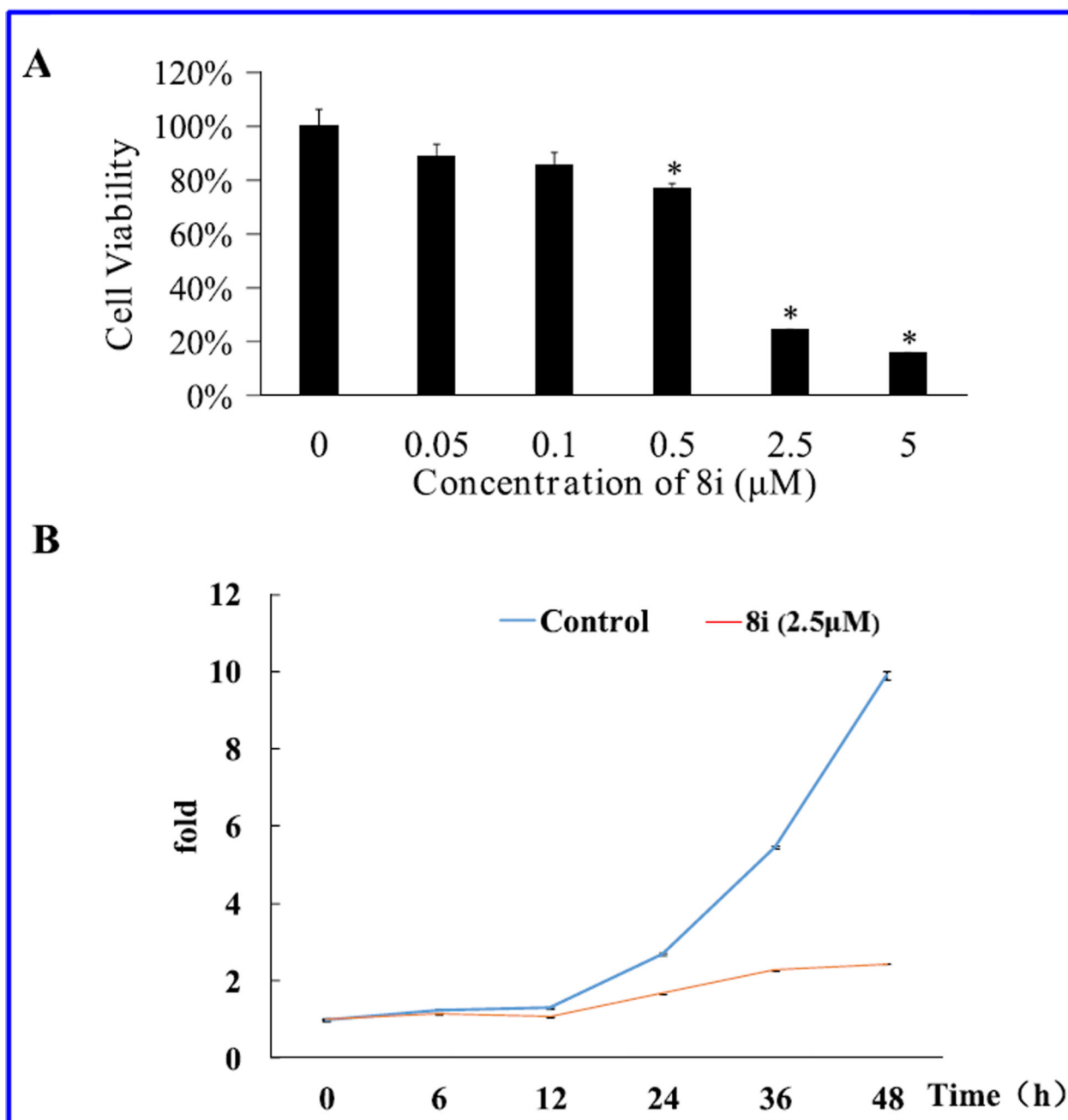
**Fig. 2.**  
Dithiocarbamate derivatives with anticancer activity.



**Fig. 3.**  
Rational molecular hybridization strategy for target antiproliferative derivatives.

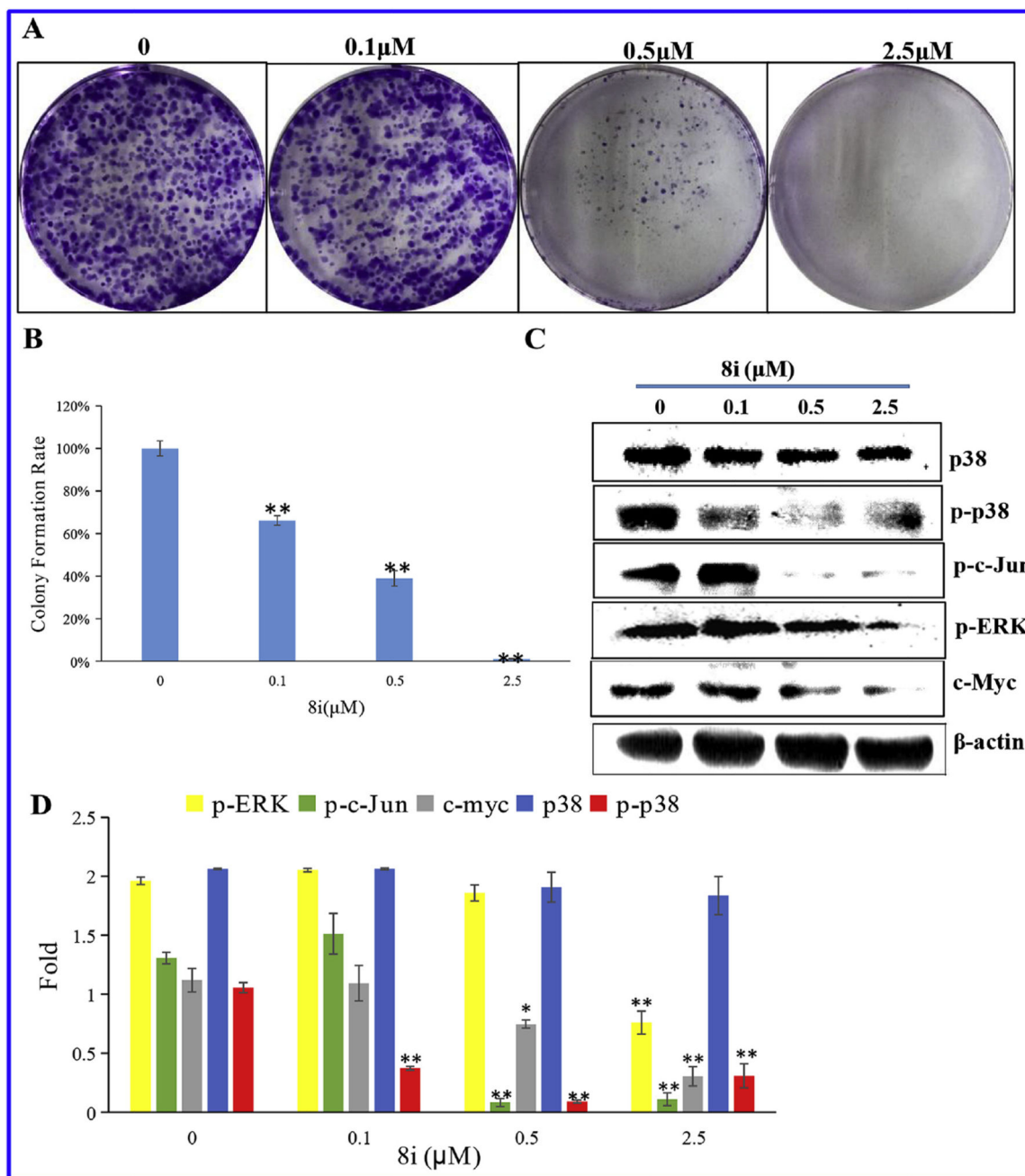


**Fig. 4.**  
Summary of SAR of target derivatives.

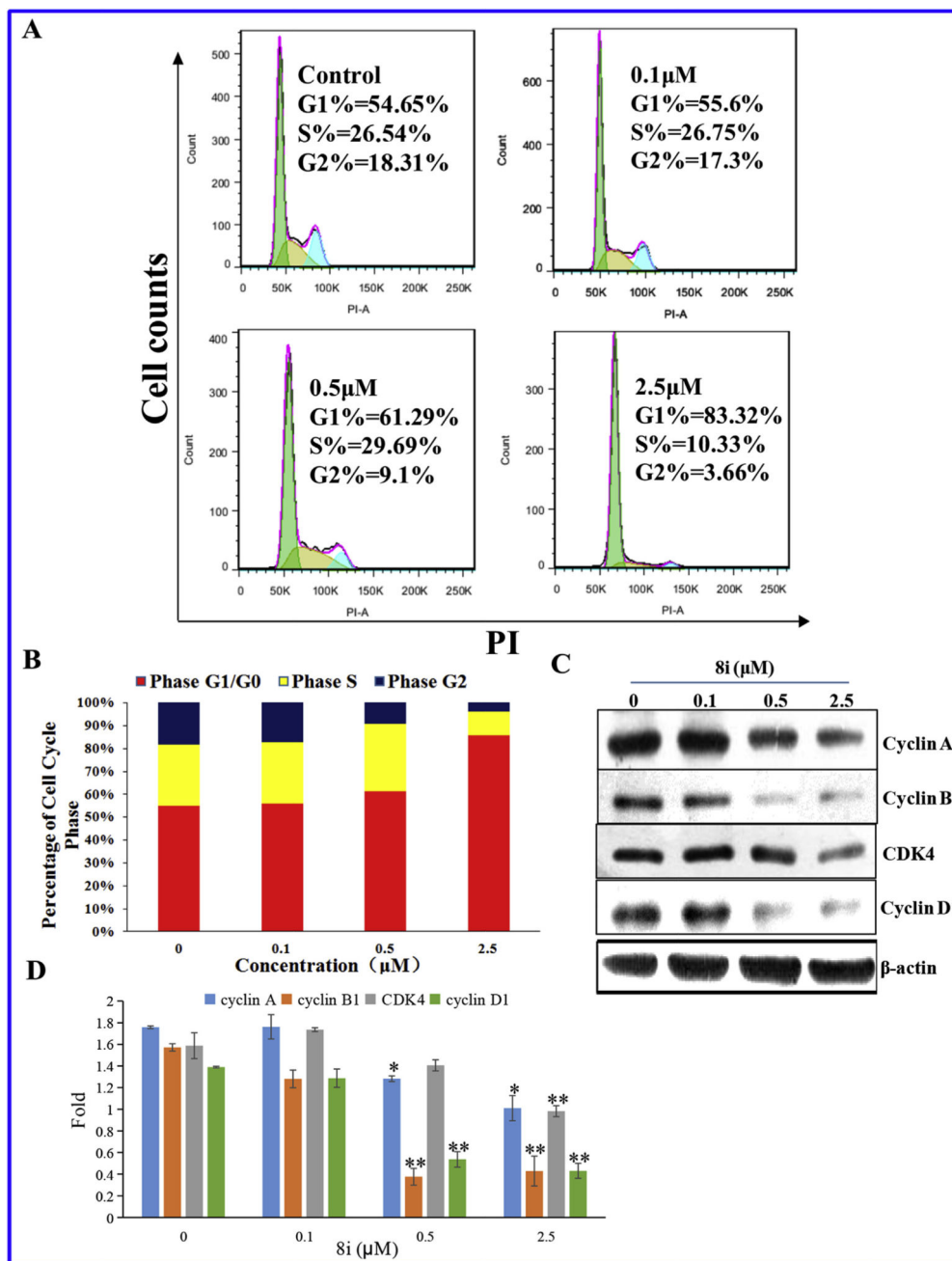


**Fig. 5.**

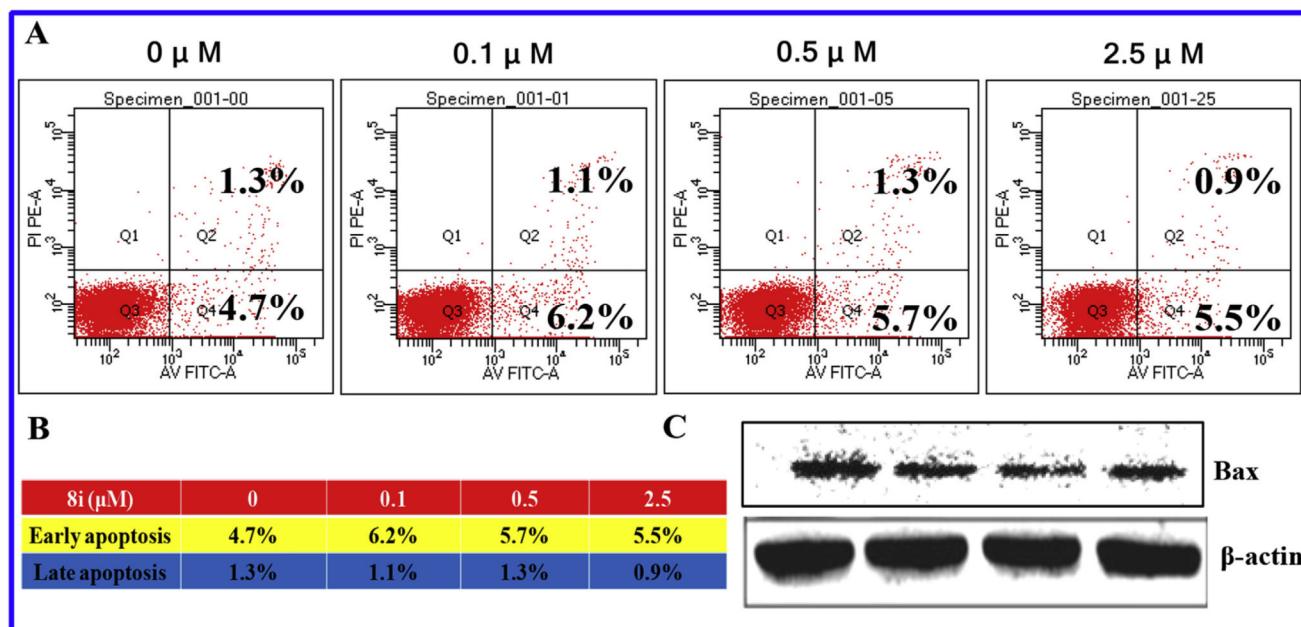
(A) The effect of **8i** in reducing cell viabilities of PC-3 cells measured by MTT assay. The cells were treated with the indicated concentrations of **8i** for 48 h. The columns of each index have \*  $p < 0.01$  vs. untreated group; (B) Growth curve of PC-3 cells.  $2.5 \times 10^4$  cells were seeded in 24-well plate. After 24 h, they were treated with **8i** (2.5  $\mu\text{M}$ ) for various time. The cell growth curve was plotted with culture time as the X axis and the fold of cell numbers gained from MTT assay as the Y axis.



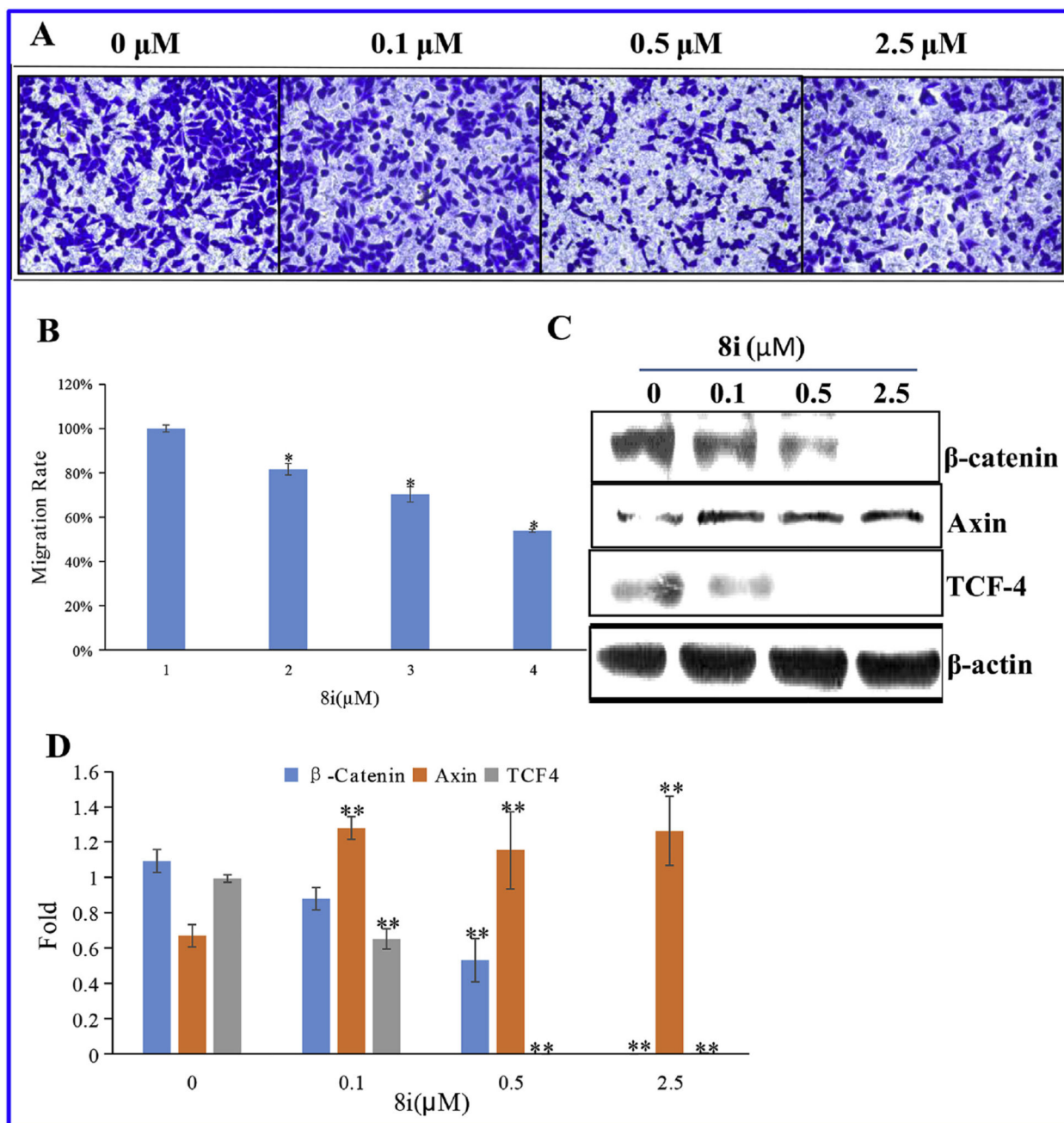
**Fig. 6.** (A) Representative images of PC-3 cells colonies after treatment with various concentrations for a week; (B) Quantitative analysis of the colony formation efficiency. The results shown were representative of three independent experiments. \*\*:  $p < 0.01$  verse control. (c) Inhibition of MAPK signaling pathway; (D) Statistical analysis of MAPK pathway protein expression levels. The results shown were representative of three independent experiments. \*:  $p < 0.05$  verse control, \*\*:  $p < 0.01$  verse control.



**Fig. 7.** (A) Effects of **8i** on PC-3 cell cycle progress for 48 h; (B) Quantitative analysis of the percentage of cell cycle phase; (C) Effects of **8i** on G1 regulatory protein. PC-3 cells were treated for 48 h with the indicated concentration of **8i**. The cells were harvested and lysed for the detection of cyclin A, cyclin B1, CDK4, cyclin D1; (D) Statistical analysis of G1 regulatory protein expression levels. The results shown were representative of three independent experiments. \*:  $p < 0.05$  verse control, \*\*:  $p < 0.01$  verse control.

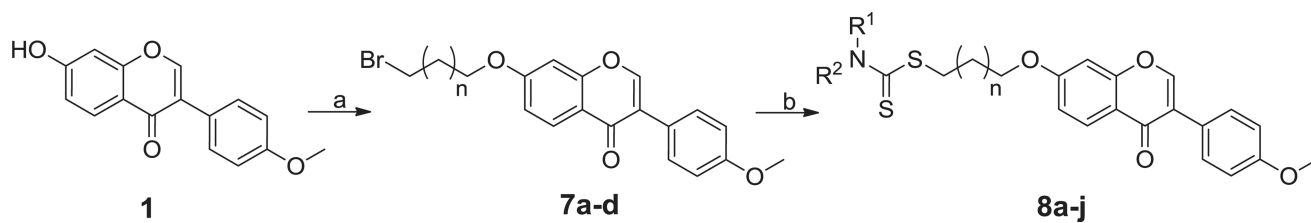


**Fig. 8.** Compound **8i** could not induce apoptosis of PC-3 cells. (A) Apoptosis analysis with PI staining after 48 h in PC-3 cells; (B) Quantitative analysis of the percentage of early apoptosis and late apoptosis; (C) Western blot analysis of Bax protein.



**Fig. 9.** Migration inhibition induced by compound **8i**. (A) Anti-migration effect of compound **8i** on PC-3 cells at concentrations of 0, 0.1, 0.5 and 2.5  $\mu\text{M}$  via transwell migration assay; (B) Quantitative analysis of migration rate; (C) Inhibition of Wnt signaling pathway; (D) Statistical analysis of Wnt pathway protein expression levels. The results shown were representative of three independent experiments. \*\*:  $p < 0.01$  verse control.

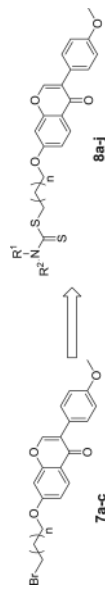


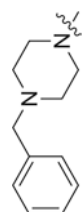
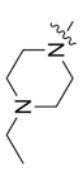
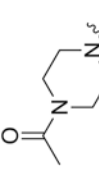
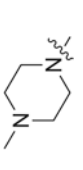
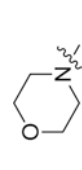
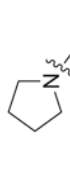
**Scheme 1.**

Reagents and conditions: (a) 1,2-dibromoethane, 1,3-dibromopropane, 1,4-dibromobutane, or 1,5-dibromopentane, K<sub>2</sub>CO<sub>3</sub>, THF, reflux, 70–83% yield; (b) CS<sub>2</sub>, substituted amine, Na<sub>3</sub>PO<sub>4</sub>·12H<sub>2</sub>O, acetone, rt, 78–85% yield.

Table 1

Antiproliferative activity of formononetin-dithiocarbamate derivatives.



Compound	R <sup>1</sup> R <sup>2</sup> , N	n <sup>a</sup>	IC <sub>50</sub> (mM) <sup>b</sup>		
			MGC-803	EC-109	PC-3
7a	-	0	>100	55.05 ± 3.98	41.89 ± 0.53
7b	-	1	64.87 ± 0.82	39.67 ± 1.14	62.61 ± 0.80
7c	-	2	52.72 ± 1.07	66.31 ± 0.75	55.62 ± 0.89
7d	-	3	>100	59.10 ± 0.81	44.76 ± 1.82
8a		1	43.81 ± 1.43	25.27 ± 0.59	14.92 ± 0.09
8b		1	53.95 ± 3.91	36.91 ± 0.67	7.08 ± 0.74
8c		1	39.42 ± 1.87	24.68 ± 1.36	4.31 ± 0.98
8d		1	21.93 ± 2.00	24.24 ± 1.16	2.21 ± 0.97
8e		1	49.62 ± 2.07	34.04 ± 0.95	27.36 ± 1.29
8f		1	39.97 ± 1.84	30.79 ± 0.73	19.36 ± 2.03

Compound	R <sup>1</sup>	R <sup>2</sup>	n <sup>a</sup>	IC <sub>50</sub> (mM) <sup>b</sup>		
				MGC-803	EC-109	PC-3
8g			1	42.02 ± 1.39	38.28 ± 0.91	17.39 ± 0.27
8h			0	11.61 ± 0.46	4.09 ± 0.83	3.64 ± 0.90
8i			1	6.07 ± 0.88	3.54 ± 1.47	1.97 ± 0.01
8j			2	31.27 ± 1.15	8.84 ± 1.27	4.61 ± 1.21
<b>1</b>	-	-	-	>100	>100	57.01 ± 1.04
<b>5-FU</b>	-	-	-	7.21 ± 1.04	10.30 ± 0.83	29.31 ± 1.87

<sup>a</sup>"n" represents the number of -CH<sub>2</sub>-.

<sup>b</sup> Antiproliferative activity was assayed by exposure for 48 h to substances and expressed as concentration required to inhibit tumor cell proliferation by 50% (IC<sub>50</sub>). Data are presented as the means ± SDs from the dose-response curves of three independent experiments.